Self-assembly route for photonic crystals with a bandgap in the visible region

ANTTI-PEKKA HYNNINEN[1,2]*, JOB H. J. THIJSSEN[2], ESTHER C. M. VERMOLEN[2], MARJOLEIN DIJKSTRA[2] AND ALFONS VAN BLAADEREN[2]*

[1]Department of Chemical Engineering, Princeton University, Princeton, New Jersey 08544-5263, USA
[2]Soft Condensed Matter, Debye Institute, Utrecht University, Princetonplein 5, 3584 CC Utrecht, The Netherlands
*e-mail: hynninen@princeton.edu; a.vanblaaderen@phys.uu.nl

Published online: 11 February 2007; doi:10.1038/nmat1841

Three-dimensional photonic crystals, or periodic materials, that do not allow the propagation of photons in all directions with a wavelength in the visible region have not been experimentally fabricated, despite there being several potential structures and the interesting applications and physics that this would lead to[1]. We show using computer simulations that two structures that would enable a bandgap in the visible region, diamond and pyrochlore, can be self-assembled in one crystal structure from a binary colloidal dispersion. In our approach, these two structures are obtained as the large (Mg) and small (Cu) sphere components of the colloidal analogue of the $MgCu_2$ Laves phase[2], whose growth can be selected and directed using appropriate wall patterning. The method requires that the particles consist of different materials, so that one of them can be removed selectively after drying (for example, by burning or dissolution). Photonic calculations show that gaps appear at relatively low frequencies indicating that they are robust and open for modest contrast, enabling fabrication from more materials.

The currently known clear champion structures, both for opening up a bandgap at the lowest refractive-index contrast ratio (around 2) and the largest bandgap width-to-frequency ratio, are dielectric diamond[3,4] and pyrochlore (also known as 'tetrastack')[5,6] structures. Both of these structures also give rise to gaps at low-lying bands, which makes them more stable against disorder[7]. Conventional methods such as lithography, and less conventional ones such as three-dimensional holographic interference lithography and two-photon lithography, have not realized these structures for a bandgap in the visible region as this requires three-dimensional feature sizes of just a few hundred nanometres. This size range is easily achieved with colloidal particles. Many other possible structures, such as inverse face-centred cubic (f.c.c.) structures, require a contrast that is too high for materials that are non-lossy in the visible region. Therefore, recently, several methods to realize structures with diamond symmetry by self-organization of colloids have been proposed. However, they require complicated[8] and/or non-spherical potentials[9] that are yet to be realized experimentally. Although it has been proposed[6,10] to use four spheres combined in the form of tetrahedrons to arrive at diamond and pyrochlore structures, the fabrication process is not described. Garcia-Adeva[5] proposed making pyrochlore lattices using a layer-by-layer growth procedure[11], which is a laborious route. Here, we show how both the pyrochlore and diamond structures can be obtained from a binary mixture of colloidal spheres with easily realizable interaction potentials. The removal of the large or small spheres from the so-called Laves phase[2] $MgCu_2$ can be done using well-established procedures, such as dissolution[12] or burning[11].

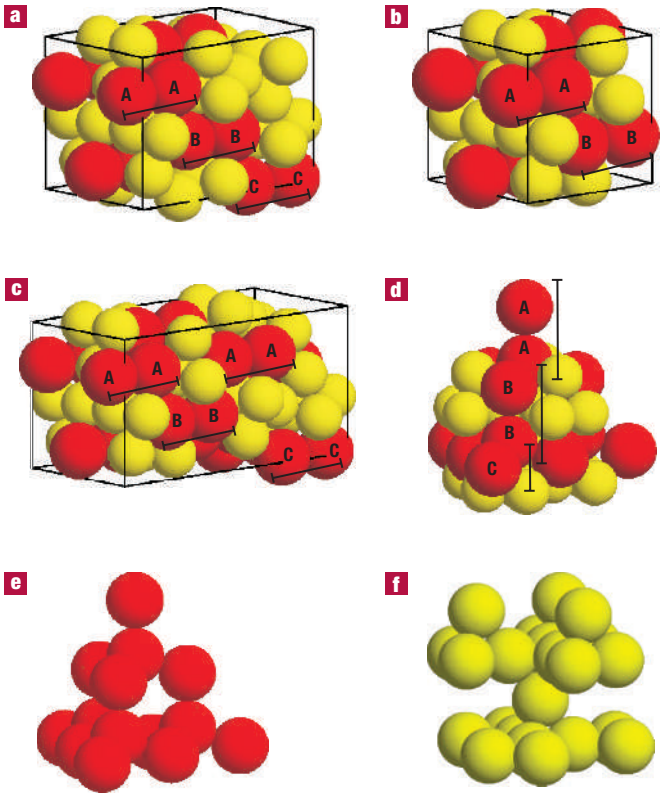

Figure 1 Binary Laves crystal structures. Large spheres are red and small spheres are yellow. **a**, $MgCu_2$. **b**, $MgZn_2$. **c**, $MgNi_2$. **d–f**, The $MgCu_2$ structure (**d**) is a combination of a diamond structure of large spheres (**e**) and a pyrochlore structure of small spheres (**f**).

$MgCu_2$ is one of three binary Laves structures[2] shown in Fig. 1. In the $MgCu_2$ structure, shown in Fig. 1a, the large spheres form

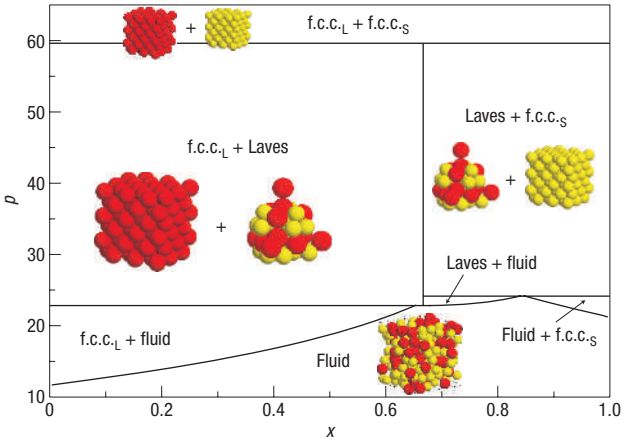

Figure 2 Phase diagram of binary hard spheres with a small-to-large size ratio of 0.82. The phase diagram is shown in the composition x, reduced pressure p, representation, where $x = N_S/(N_S + N_L)$ is the number fraction of small spheres. The labels 'f.c.c.$_L$' and 'f.c.c.$_S$' denote the f.c.c. crystals of large and small particles, respectively. The phase coexistence regions are labelled 'f.c.c.$_L$ + Laves', 'Laves + f.c.c.$_S$' and so on.

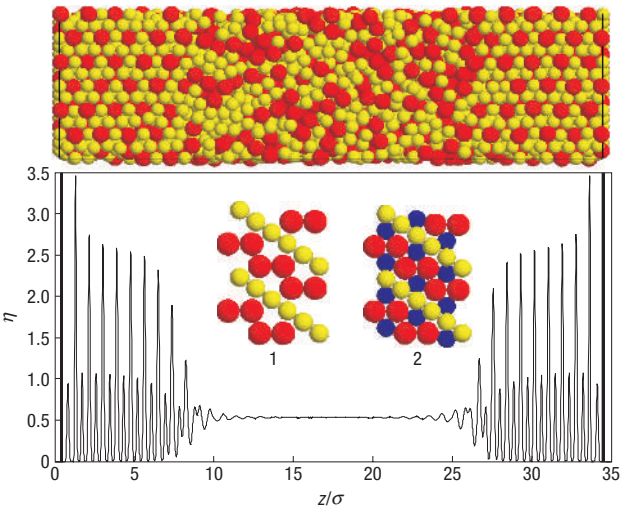

Figure 3 Density profile and a snapshot of the simulation along the z direction. Structure 1: Small (yellow) and large (red) spheres attached to a wall resembling the (110) plane of the $MgCu_2$ structure. Structure 2: Wall pattern plus the first plane of mobile small spheres (dark blue) slightly above the wall.

two interpenetrating f.c.c. lattices, whereas the small spheres sit at the vertices of a tetrahedron. As indicated in Fig. 1a, the stacking of large sphere pairs in $MgCu_2$ is AABBCC. In $MgZn_2$, shown in Fig. 1b, the stacking of large spheres is AABB, and in $MgNi_2$, shown in Fig. 1c, the stacking is AABBAACC. The diamond structure, shown in Fig. 1e, is obtained from $MgCu_2$ (Fig. 1d) by removing the small spheres, whereas the pyrochlore structure, shown in Fig. 1f, is obtained by removing the large spheres. The maximum packing fraction of $MgCu_2$ (and other Laves) phases $\eta \approx 0.710$ is achieved at the small-to-large sphere diameter ratio $\sigma_S/\sigma_L = \sqrt{2/3} \approx 0.82$. At the maximum packing, both the diamond and the pyrochlore component crystals are at their maximum packing fractions of 34% and 37%, respectively, and are thus self-supporting.

Figure 2 shows the phase diagram of binary hard spheres with a size ratio of 0.82 in the reduced pressure $p = P\sigma_L^3/kT$, composition x presentation, where $x = N_S/(N_S + N_L)$ is the number fraction of small spheres, k is Boltzmann's constant and T is the absolute temperature. The phase diagram is obtained from Gibbs free-energy data, where the free energies of the Laves phases are calculated using Monte Carlo (MC) simulations[13] and the free energies of the fluid and f.c.c. phases are taken from analytical results[14,15]. The phase diagram consists mainly of coexistence regions where the tie lines are horizontal. For example, in the region marked 'f.c.c.$_L$ + Laves', the stable system has an f.c.c. crystal of large spheres at $x = 0$ in coexistence with Laves structures at $x = 2/3 = 0.667$. The pure one-phase regions are at $x = 0$, $x = 2/3$, $x = 1$ and in the fluid phase. The phase diagram can also be drawn, for example, in the packing fraction η, composition x plane, where the pressure region $p = 22.8$–59.6 of stable Laves structures corresponds to packing fractions $\eta = 0.59$–0.66.

We found the Laves structures to be stable at size ratios in the 0.74–0.84 range. Thus, the main features of the phase diagram in Fig. 2 are expected to hold in this size-ratio range. The addition of soft repulsion (screened Coulomb) to the interparticle potential shifted the stability range to lower size ratios. This is in agreement with experiments on charged colloids, where indications for both $MgCu_2$ and $MgZn_2$ structures were reported in the size-ratio range 0.59–0.71 (refs 16–18). Recently, the Laves structures $MgZn_2$ and $MgNi_2$ have also been observed in experiments with binary nanoparticle suspensions[19].

The relative stability of the three different Laves structures was studied by calculating their Helmholtz free energies[13] with extrapolation to the infinite-system limit[20]. As all of the Laves structures pack with the same volume fraction (η), it is not surprising that the free-energy difference between them turned out to be very small, of the order of 10^{-3} kT per particle (at $\eta = 0.6$ and a size ratio of 0.82). Owing to the small free-energy differences between the Laves structures, we expect to observe a mix of all three structures in experiments, analogously to single-sized hard spheres where, instead of a pure f.c.c. or hexagonal close-packed, a random hexagonal close-packed crystal is observed[21]. Fortunately, the $MgCu_2$ crystal structure can be selected to grow in pure form by, for instance, templating the wall using the pattern shown in Fig. 3 (structure 1), which resembles the (110) plane of the $MgCu_2$ structure. The template is not exactly the (110) plane, as the large and small spheres were placed touching the wall, as they would be in an experimental situation where particles are placed on the wall by, for example, optical tweezers[22]. The first layer of mobile small particles is shown in Fig. 3 (structure 2) by the dark blue spheres. The density was set to $\eta = 0.555$, which is below $MgCu_2$ bulk freezing density ($\eta = 0.59$). The particle distances in the template correspond to $\eta = 0.59$. MC simulations were done in the canonical ensemble in a system with 4,077 particles, patterned walls at $z = 0$ and $z = 35\sigma_L$ and periodic boundaries in the other two directions. Figure 3 shows a snapshot of the system and the equilibrium density profile along the z direction. We observe that there are 8–7 crystalline layers close to both walls and a homogeneous bulk-like fluid phase in the middle at a volume fraction $\eta = 0.533 \pm 0.005$. For conditions above the $MgCu_2$ bulk freezing density, we expect larger crystals and no fluid phase. In a similar way, for single hard-sphere dispersions, the growth of metastable hexagonal close-packed crystals of millimetre size has been demonstrated experimentally with a templated wall[23].

Figure 4 shows the relative width of the photonic bandgap between bands 2 and 3, as a function of the dielectric contrast, for the direct diamond and pyrochlore structures (dielectric spheres

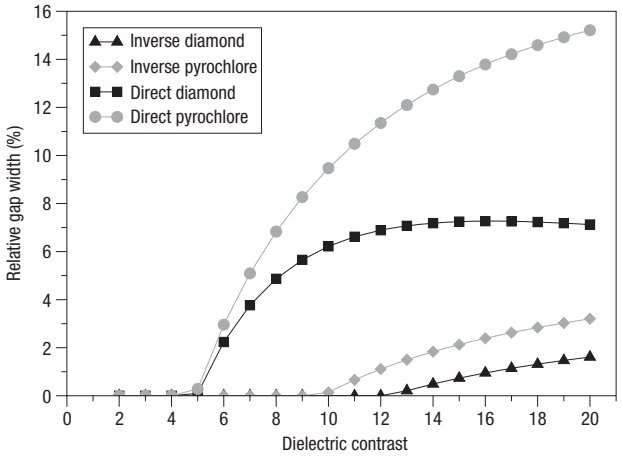

Figure 4 Calculated relative width of the gap between bands 2 and 3 as a function of the dielectric contrast. Four different structures are considered: direct pyrochlore ($\eta = 0.37$), direct diamond ($\eta = 0.34$) (dielectric spheres in air), and inverse pyrochlore and inverse diamond (air spheres in a dielectric background). The relative gap width is defined as the gap width divided by the midgap frequency. The solid lines are guides for the eye.

in air), and their inverse structures (air spheres in a dielectric background), at the maximum sphere packing fraction. The direct structures in particular possess large photonic bandgaps for moderate dielectric contrasts. Their gap opens up at a dielectric contrast of 5, which is much lower than the required contrast of 8.4 for an inverse f.c.c. structure[24]. At a contrast of 12 (silicon spheres in air), the gap width has increased to approximately 7% and 11% for the direct diamond and direct pyrochlore structures, respectively. These gaps are much larger and open up at lower contrasts than for the inverse structures. We did not find any bandgaps for the binary Laves structures. Neither did we find any significant gaps for the small/large particle components of the $MgZn_2$ and $MgNi_2$ structures.

Photonic band diagrams were calculated up to band 10 for dielectric contrasts ranging from 2 to 20 using $32 \times 32 \times 32$ grid points to discretize the unit cell, using the MIT Photonic-Bands (MPB) software package[25]. This software computes fully vectorial eigenmodes of Maxwell's equations with periodic boundary conditions by preconditioned conjugate-gradient minimization of the block Rayleigh quotient in a plane-wave basis[25]. We checked the convergence of the MPB calculations for diamond and pyrochlore using the photonic analogue of the Koringa–Kohn–Rostoker (KKR) method[4,26,27] and found that MPB and KKR agree on the midgap frequency of the gap between bands 2 and 3, and on the dielectric contrast at which the gap opens, but not always on the gap width.

We emphasize that the structures for which the large gaps are calculated have not been optimized in any way. This optimization might be achieved, for instance, by using incomplete filling, which increases gaps for inverse f.c.c. structures[28], or by slightly sintering the structures[29]. Nevertheless, as shown in Fig. 4, several low-dielectric-constant materials, such as titania[30] and zinc sulphide[31], could open a gap in the visible region for close-packed diamond and pyrochlore structures. Particles made of these materials, which are non-lossy and have a high enough refractive index, could be combined with polystyrene and poly(methyl methacrylate) particles in binary colloidal crystals, similar to what has already been demonstrated in combination with silica particles[11,32]. Although we have focused here on pure dielectric materials, interesting possibilities also exist for structures consisting of metallodielectric spheres[4].

In summary, we have proposed a method to fabricate photonic crystals with a diamond or pyrochlore structure through self-assembly of the $MgCu_2$ structure using a binary mixture of colloidal spheres. Our method requires standard techniques: the preparation of two species of colloidal spheres (charged or hard sphere), surface patterning and the removal of one of the species. Therefore, it is a promising route for the experimental realization of photonic crystals with a bandgap in the visible region.

METHODS

The phase diagram in Fig. 1 was constructed from Gibbs free-energy data using the common tangent construction in the (Gibbs free energy G, composition x)-plane. Gibbs free energies were obtained from the sum of the Helmholtz free energy F and the equation of state as $G = F + PV$, where V is volume. For the $MgCu_2$ structure, Helmholtz free energies and the equation of state were calculated numerically. The numerical calculations were done for a system with $N_L = 64$ and $N_S = 128$ particles in a cubic box with periodic boundary conditions. The free-energy calculations were done using the harmonic coupling method and consisted of 10 integration steps selected according to Gauss–Legendre quadrature[13]. At each step the system was first equilibrated during 5×10^4 MC steps (trials to displace each particle) in the canonical ensemble and then sampled during 10^5 MC steps. For the purpose of extrapolation to the infinite-system-size limit, system sizes up to $N_L = 1{,}920$ and $N_S = 3{,}840$ particles were used. The equation of state of $MgCu_2$ was calculated in the isobaric–isothermal ensemble, where the average volume was calculated using 2×10^5 equilibration steps and 4×10^5 sampling steps. A smooth function for the equation of state was obtained by fitting the data using a linear combination of the functions $1/\gamma(\eta)$, 1, $\gamma(\eta)$, $\gamma(\eta)^2, \ldots$ where $\gamma(\eta) = \eta_{cp}/\eta - 1$ and η_{cp} is the maximum packing of $MgCu_2$ ($\eta_{cp} \approx 0.710$ for $\sigma_S/\sigma_L = 0.82$). The density profile in Fig. 3 was calculated for $N_L = 1{,}359$ and $N_S = 2{,}718$ particles in a box with dimensions $(8.52\sigma_L, 9.05\sigma_L, 34.95\sigma_L)$ using 4.1×10^8 equilibration steps and 10^7 sampling steps.

Photonic band diagrams were calculated using the MPB package, version 1.4.2. In addition, an MPB patch file by Mischa Megens was installed for calculating the effective dielectric constant by averaging over Wigner–Seitz cells rather than over the parallelepipeds spanned by the lattice vectors. This patch also ensures proper weighting of the dielectric constant at the edges of the unit cell, and thus avoids double-counting.

Received 26 October 2006; accepted 18 December 2006; published 11 February 2007.

References

1. Soukoulis, C. M. (ed.) *Photonic Crystals and Light Localization in the 21st Century* (NATO Science Series (C): Mathematical and Physical Sciences, Kluwer Academic, Dordrecht, 2001).
2. Pearson, W. B. *The Crystal Chemistry and Physics of Metals and Alloys* (Wiley-Interscience, New York, 1972).
3. Maldovan, M., Ullal, C. K., Carter, W. C. & Thomas, E. L. Exploring for 3D photonic bandgap structures in the 11 f.c.c. space groups. *Nature Mater.* **2**, 664–667 (2003).
4. Moroz, A. Metallo-dielectric diamond and zinc-blende photonic crystals. *Phys. Rev. B* **66**, 115109 (2002).
5. Garcia-Adeva, A. J. Band gap atlas for photonic crystals having the symmetry of the kagome and pyrochlore lattices. *New J. Phys.* **8**, 86 (2006).
6. Ngo, T. T., Liddell, C. M., Ghebrebrhan, M. & Joannopoulos, J. D. Tetrastack: colloidal diamond-inspired structure with omnidirectional photonic band gap for low refractive index. *Appl. Phys. Lett.* **88**, 241920 (2006).
7. Li, Z.-Y. & Zhang, Z.-Q. Fragility of photonic band gaps in inverse-opal photonic crystals. *Phys. Rev. B* **62**, 1516–1519 (2000).
8. Tkachenko, A. V. Morphological diversity of DNA-colloidal self-assembly. *Phys. Rev. Lett.* **89**, 148303 (2002).
9. Zhang, Z., Keys, A. S., Chen, T. & Glotzer, S. C. Self-assembly of patchy particles into diamond structures through molecular mimicry. *Langmuir* **21**, 11547–11551 (2005).
10. Manoharan, V. N. & Pine, D. J. Building materials by packing spheres. *Mater. Res. Soc. Bull.* **29**, 91–95 (2004).
11. Velikov, K. P., Christova, C. G., Dullens, R. P. A. & van Blaaderen, A. Layer-by-layer growth of binary colloidal crystals. *Science* **296**, 106–109 (2002).
12. Vlasov, Y. A., Bo, X. Z., Sturm, J. C. & Norris, D. J. On-chip natural assembly of silicon photonic bandgap crystals. *Nature* **414**, 289–293 (2001).
13. Frenkel, D. & Smit, B. *Understanding Molecular Simulations* (Academic, New York, 2002).
14. Mansoori, G. A., Carnahan, N. F., Starling, K. E. & Leland, T. W. Jr. Equilibrium thermodynamic properties of the mixture of hard spheres. *J. Chem. Phys.* **54**, 1523–1525 (1971).
15. Speedy, R. J. Pressure and entropy of hard-sphere crystals. *J. Phys. Condens. Matter* **10**, 4387–4391 (1998).

16. Hasaka, M., Nakashima, H. & Oki, K. Structure of the Laves phase observed in polystyrene latexes. *Trans. Japan Inst. Met.* **25**, 65–72 (1984).
17. Yoshimura, S. & Hachisu, S. Order formation in binary mixtures of monodisperse latices. *Prog. Colloid Polym. Sci.* **68**, 59–70 (1983).
18. Ma, G. H., Fukutomi, T. & Morone, N. Preparation and analysis of ordered structure of binary-mixtures composed of poly(4-vinylpyridine) and polystyrene microgels. *J. Colloid Interface Sci.* **168**, 393–401 (1994).
19. Shevchenko, E. V., Talapin, D. V., Kotov, N. A., O'Brien, S. & Murray, C. B. Structural diversity in binary nanoparticle superlattices. *Nature* **439**, 55–59 (2006).
20. Polson, J. M., Trizac, E., Pronk, S. & Frenkel, D. Finite-size corrections to the free energies of crystalline solids. *J. Chem. Phys.* **112**, 5339–5342 (2000).
21. Pusey, P. N. *et al.* Structure of crystals of hard colloidal spheres. *Phys. Rev. Lett.* **63**, 2753–2756 (1989).
22. Hoogenboom, J. P., Vossen, D. L. J., Faivre-Moskalenko, C., Dogterom, M. & van Blaaderen, A. Patterning surfaces with colloidal particles using optical tweezers. *Appl. Phys. Lett.* **80**, 4828–4830 (2002).
23. Hoogenboom, J. P., van Langen-Suurling, A. K., Romijn, J. & van Blaaderen, A. Hard-sphere crystals with hcp and non-close-packed structure grown by colloidal epitaxy. *Phys. Rev. Lett.* **90**, 138301 (2003).
24. Biswas, R., Sigalas, M. M., Subramania, G. & Ho, K.-M. Photonic band gaps in colloidal systems. *Phys. Rev. B* **57**, 3701–3705 (1998).
25. Johnson, S. G. & Joannopoulos, J. D. Block-iterative frequency-domain methods for Maxwell's equations in a planewave basis. *Opt. Express* **8**, 173–190 (2001).
26. Wang, X., Zhang, X.-G., Yu, Q. & Harmon, B. N. Multiple-scattering theory for electromagnetic-waves. *Phys. Rev. B* **47**, 4161–4167 (1993).
27. Moroz, A. Density-of-states calculations and multiple-scattering theory for photons. *Phys. Rev. B* **51**, 2068–2081 (1995).
28. Busch, K. & John, S. Photonic band gap formation in certain self-organizing systems. *Phys. Rev. E* **58**, 3896–3908 (1998).
29. Miguez, H. *et al.* Control of the photonic crystal properties of fcc-packed submicrometer SiO_2 spheres by sintering. *Adv. Mater.* **10**, 480–483 (1998).
30. Eiden-Assmann, S., Widoniak, J. & Maret, G. Synthesis and characterization of porous and nonporous monodisperse colloidal TiO_2 particles. *Chem. Mater.* **16**, 6–11 (2004).
31. Velikov, K. P. & van Blaaderen, A. Synthesis and characterization of monodisperse core-shell colloidal spheres of zinc sulfide and silica. *Langmuir* **17**, 4779–4786 (2001).
32. Leunissen, M. E. *et al.* Ionic colloidal crystals of oppositely charged particles. *Nature* **437**, 235–240 (2005).

Acknowledgements

We thank M. Megens for the MPB patch file and A. Moroz for useful discussions on KKR calculations and for providing the FORTRAN KKR code. This work is part of the research program of the 'Stichting voor Fundamenteel Onderzoek der Materie (FOM)', which is financially supported by the 'Nederlandse Organisatie voor Wetenschappelijk Onderzoek (NWO)'. The work of E.C.M.V. is supported by NanoNed, a nanotechnology program of the Dutch Ministry of Economic Affairs. This work has been carried out within the framework of the SFB TR6 Collaborative Research Centre. On its inducement, it has been printed under appropriation of funds that were set at disposal by the DFG. Correspondence and requests for materials should be addressed to A.-P.H. or A.v.B.

Author contributions

A.-P.H. did the MC simulations under the supervision of M.D., J.H.J.T and E.C.M.V did the photonic bandgap calculations and A.v.B. initiated and supervised the project.

Competing financial interests

The authors declare that they have no competing financial interests.